Food Research International 147 (2021) 110527

Contents lists available at ScienceDirect

Food Research International

journal homepage: www.elsevier.com/locate/foodres

Skimmed milk structural dynamics during high hydrostatic pressure processing from *in situ* SAXS

Shuailing Yang [a], Arwen I.I. Tyler [b], Lilia Ahrné [a,*], Jacob J.K. Kirkensgaard [a,c,*]

[a] Department of Food Science, University of Copenhagen, DK-1958 Frederiksberg C, Denmark
[b] School of Food Science and Nutrition, University of Leeds, LS2 9JT Leeds, United Kingdom
[c] Niels Bohr Institute, University of Copenhagen, DK-2100 København Ø, Denmark

ARTICLE INFO

Keywords:
Casein micelle
Multiple high-pressure processing
Colloidal calcium phosphate (CCP)
Small-angle X-ray scattering (SAXS)
Protein structure modification

ABSTRACT

Understanding the changes in milk at a nanostructural level during high-pressure (HP) treatment can provide new insights to improve the safety and functionality of dairy products. In this study, modifications of milk nanostructure during HP were studied *in situ* by small-angle X-ray scattering (SAXS). Skimmed milk was pressurized to 200 or 400 MPa at 25, 40 or 60 °C and held for 5 or 10 min, and the effect of single- and double-HP treatment was also investigated. In most cases, the SAXS patterns of skimmed milk are well fitted with a three-population model: a low-q micellar feature reflecting the overall micelle size (~0.002 $Å^{-1}$), a small casein cluster contribution at intermediate-q (around 0.01 $Å^{-1}$) and a high-q (0.08–0.1 $Å^{-1}$) population of milk protein inhomogeneities. However, at 60 °C a scattering feature of colloidal calcium phosphate (CCP) which is normally only seen with neutron scattering, was observed at 0.035 $Å^{-1}$. By varying the pressure, temperature, holding and depressurization times, as well as performing cycled pressure treatment, we followed the dynamic structural changes in the skimmed milk protein structure at different length scales, which depending on the processing conditions, were irreversible or reversible within the timescales investigated. Pressure and temperature of the HP process have major effects, not only on size of casein micelles, but also on "protein inhomogeneities" within their internal structure. Under HP, increasing processing time at 200 MPa induced re-association of the micelles, however, the changes in the internal structure were more pressure-dependent than time dependent.

1. Introduction

Milk is a water-based complex fluid having characteristic structures at different length-scales (Peyronel, Marangoni, & Pink, 2020). The continuous phase in milk consists of whey proteins, carbohydrates and soluble ions, where the fat globules (Lopez et al., 2011), and the casein micelles are dispersed (Dalgleish & Corredig, 2012). In skimmed milk, the colloidal globular micelles of casein are the predominant component, and its structure contributes to the major physicochemical and organoleptic properties of milk, such as the color, texture and mouthfeel (Boukria et al., 2020). Although the structure of casein micelles has been studied extensively, the exact model for its fine structure assembly and especially their changes during processing is still elusive (Walstra, 1999; Ingham et al., 2016; Day, Raynes, Leis, Liu, & Williams, 2017).

Todaýs consumers are demanding nutritious and fresh-like foods, and in this respect non-thermal processing technologies, such as high-pressure (HP) have shown to provide significant advantages *e.g.* less nutritional and flavour losses, while also providing more sustainable products due to the extension of their shelf-life. However, the pressure required to produce milk with suitable microbial quality has been shown to cause modifications in milk proteins and sensory attributes (Liu, Carøe, Qin, Munk, Crafack, Petersen & Ahrné, 2020). In the past decades, the effects of HP processing on milk components have been thoroughly studied and reviewed (Huppertz, Kelly, & Fox, 2002; Huppertz, Fox, de Kruif, & Kelly, 2006; López-Fandiño, 2006; Trujillo, Capellas, Saldo, Gervilla, & Guamis, 2002; Voigt, Kelly, & Huppertz, 2015) showing major modifications on the two major milk proteins, β-lactoglobulin (β-Lg) and caseins. HP processing of milk induces dissociation of casein micelles, as a consequence of increased solubility of colloidal calcium phosphate (CCP) with pressure, as well as unfolding and loss of secondary structure of β-Lg, exposing free thiol groups which promotes oligomerization and aggregation with other proteins. Depending on the applied HP conditions, some of these changes are reversible once the pressure is released (Olsen & Orlien, 2016), but limited knowledge is

* Corresponding authors.
E-mail addresses: lilia@food.ku.dk (L. Ahrné), jjkk@food.ku.dk (J.J.K. Kirkensgaard).

https://doi.org/10.1016/j.foodres.2021.110527
Received 14 January 2021; Received in revised form 27 May 2021; Accepted 11 June 2021
Available online 14 June 2021

available at a nanostructural level, which is the focus of the current work.

Small-angle X-ray scattering (SAXS) is a non-disruptive technique able to probe milk in its intact state and it allows the combination of scattering and *in situ* HP to investigate the milk micelle structure in real time (Yang, Gu, Banjar, Li, & Hemar, 2018). It was shown previously (Mata, Udabage, & Gilbert, 2011; de Kruif, 2014; Ingham et al., 2016, Smith, Brok, Christiansen, & Ahrné, 2020) that SAXS and ultra-SAXS can be used to investigate nano- and micron-sized structures in complex dairy matrixes. Milk scattering is complicated and has been a matter of controversy regarding the interpretation of the scattering data for decades. The scattering feature at intermediate-q (around 0.01 $Å^{-1}$), only observed in some samples, has been attributed to a variety of structures. Some researchers consider it to represent a separate population of scatterers such as "mini-micelles" in solution (Müller-Buschbaum, Gebhardt, Roth, Metwalli, & Doster, 2007), while others considered it to represent the internal structure of the casein micelle, consisting of "incompressible regions" of casein clusters (Ingham et al., 2016; Bouchoux, Gesan-Guiziou, Pérez, & Cabane, 2010) or "submicelles" (Yang et al., 2018). The high-q (0.08–0.1 $Å^{-1}$) feature is commonly thought to be attributed to the form factor scattering from colloidal calcium phosphate (CCP) (Marchin, Putaux, Pignon, & Léonil, 2007; Mata et al., 2011; Yang et al., 2018). However, de Kruif et al. (2014) reported that CCP scattering was several orders of magnitude lower in intensity than protein scattering and was therefore unlikely to be observable under a typical SAXS setup. They suggested that the high-q feature is related to protein inhomogeneities. Ingham et al. (2016) confirmed the conclusions made by de Kruif et al. (2014) and reported that the CCP scattering feature is at $q \sim 0.035$ $Å^{-1}$ using resonant soft X-ray scattering (RSoXS). The SAXS feature at high-q (0.08–0.1 $Å^{-1}$) mainly arises from the structure factor of proteins and the CCP scattering makes up less than 20% of the total intensity. Recently, Singh, Hemar, Gilbert, Wu, and Yang (2020) found that changing the substructure of caseins upon cross-linking with genipin, but not changing CCP levels also leads to a less prominent shoulder at $q = 0.08$ $Å^{-1}$. They also supported the normally observed high-q feature as arising from the structure factor of proteins.

Previously, Yang et al. (2018) used *in situ* synchrotron SAXS to study skim milk structural changes by applying a continuous and gradual increased HP from 160 to 960 MPa step by step (after a pressure holding for about 12 min) and reported disruption of the casein micelles into "submicelles" with increasing HP that partially reversed after pressure release. The study demonstrated the potential use of synchrotron SAXS coupled with HP to examine *in situ* and in real time the structural evolution of milk under pressure. However, they did not analyze the data with any underlying structural model as we present here. Additionally, the pressure-induced changes on caseins and their recovery depend not only on pressure but on the combined effects of pressure, time and temperature applied (Gaucheron et al., 1997, Olsen & Orlien, 2016), as well as the frequency of the HP treatments (Yang et al., 2020). Depressurisation rate may have an effect but it is more difficult to control with most of the equipment available. In the context of HP processing of milk, multiple HP cycles have shown positive effects on microbial inactivation (Cornell, 2017; Hu et al., 2015; 2017) with limited effect on caseins (Yang et al., 2020). Therefore, we hypothesize that cycled HP treatments have effects on the milk colloidal structure dynamics, which needs further investigation to support the development of new processes and equipment.

Here we investigated the skimmed milk structure dynamics during HP treatment using a more advanced *in situ* pressure cell and synchrotron SAXS (Brooks et al., 2010). The irreversibility of time-dependent nanostructural changes resulting from HP application to skimmed milk at 200 and 400 MPa at 25, 40 and 60 °C, including repeated cycles were studied here for the first time. Such a comprehensive investigation of the effect of different HP processing conditions on the milk nanostructure in skimmed milk will extend the present understanding of HP effects on milk properties and how HP modifies the milk structure, which is valuable to explore the intrinsic properties of milk for the development of new dairy products.

2. Materials and methods

2.1. Materials and sample preparation

Fresh bovine raw milk was obtained from a Danish local organic farm (Mannerup Møllegård, Osted, Denmark) and was skimmed on the same day at ~ 45 °C on a Milky FJ 130 ERR separator containing 21 discs (Janschitz GmbH, Althofen, Austria). Milk samples were transported with ice-blocks in an insulated box and stored at 4 °C, and the X-ray scattering experiments were performed on the third day. The simulated milk ultrafiltrate (SMUF) solution was freshly prepared as described by Spanos et al. (2007) and all chemicals used were of analytical grade and obtained from Sigma Chemical Co. (St. Louis, MO) or BDH Chemicals (BDH Ltd., Poole, England).

2.2. High-pressure X-ray scattering experiments

The X-ray experiments were carried out at Diamond Light Source (Didcot, UK) on beamline I22. The synchrotron X-ray beam was tuned to a wavelength of 0.69 Å. The distance between the sample and detector was set at 9.84 m and the diffraction patterns were recorded on a Pilatus 2 M detector, which results in a q-range from 2.24×10^{-3} to 0.258 $Å^{-1}$. Approximately 20 μL sample was loaded into a polycarbonate capillary (Makrolon 3158–550115, transparent, Precision Extrusion, New York, US) with a diameter of 2 mm and wall thickness of 0.05 mm. The capillary was plugged with rubber tubing and sealed with a nondrying, nonshrinking Araldite glue sealing compound (Cristaseal, Hawksley, Sussex, UK) waiting at 4 °C for ~ 2 h to let the wax solidify. Samples were inserted in a custom-built sample holder, mounted in the HP cell and subjected to various HP treatments (HP process 1–3, as shown in Fig. 1) at 200 or 400 MPa and 25, 40 or 60 °C.

The details of the sample holder and pressure cell used have been described previously by Brooks et al. (2010) and ramping to the desired pressure takes less than 15 ms with pressure oscillations of approximately ± 15 MPa. Scattering data were collected for milk before, during and after pressurization. Thus, for HP process 1 six scattering data points (P0-P5) were collected to track the milk scattering pattern variations before, under and after HP treatment. HP process 2 with 7 data collection points was only performed at 200 MPa to study the effects of HP treatment time and HP process 3 was designed as a two-cycle treatment having 7 data collection points but same total treatment time as HP process 1, to compare the effect of repeated HP treatment on the milk structure.

2.3. SAXS data reduction and analysis

The raw data were re-binned logarithmically using WillItRebin (Pedersen, Arleth, & Mortensen, 2013) executed under Python 3.8.3 with the logarithmic rebinning coefficient set as 1.04 to reduce the raw SAXS data points from 1603 to 107 points speeding up the fitting procedure. The milk SAXS data was background subtracted with the SMUF solution scattering pattern at 25 °C under ambient pressure normalized to the high-q scattering.

For the data analysis, we followed the recent paper of Ingham et al. (2016), where a detailed review of model-dependent fitting of SAXS from bovine skimmed milk was given. In the modelling, the starting point is the general equation for the scattering intensity per unit volume of a two-phase system:

$$I(q) = \Delta\rho^2 n_p V_p^2 P_p(q) S(q) \quad (1)$$

where $\Delta\rho^2$, n_p, V_p and $P_p(q)$ are the contrast, number, volume and form factor of the particle in question, respectively; q is the length of the

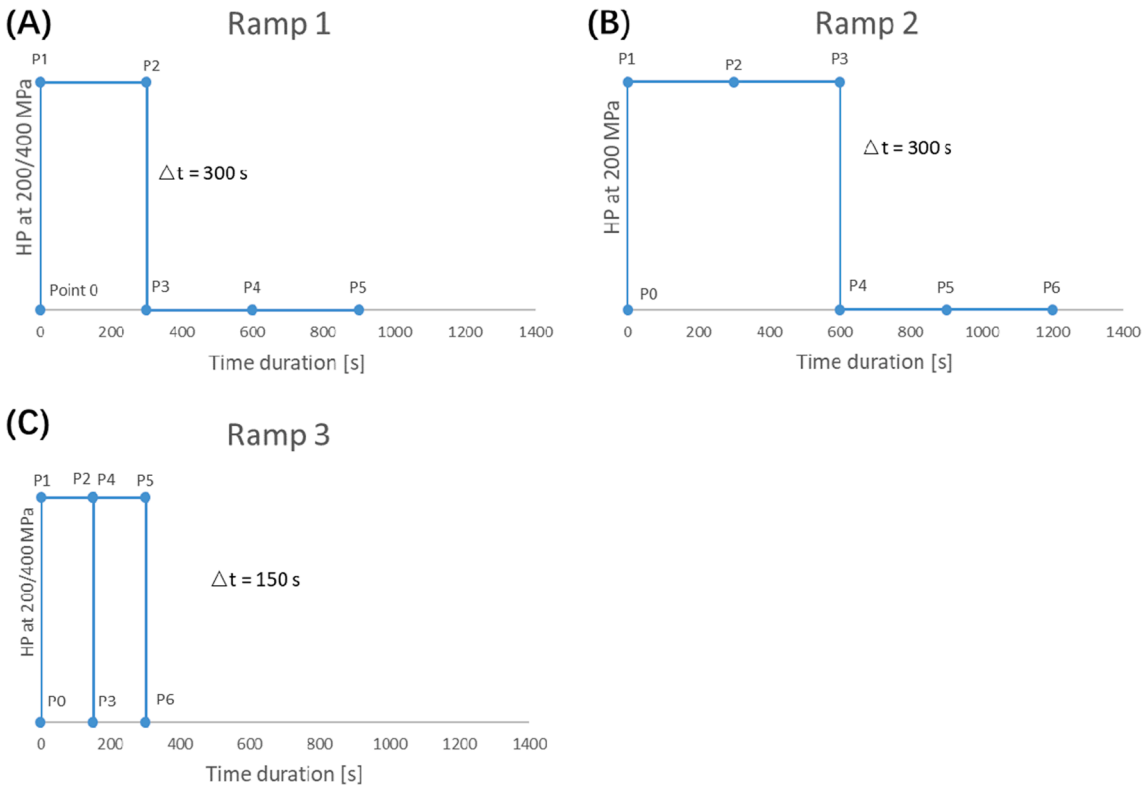

Fig. 1. Schematic of HP processes. The P# numbers indicate when SAXS data were recorded, *e.g.* at P0 the SAXS scattering of the sample before HP treatment was recorded, P1, when the pressure reached the given value (200 MPa or 400 MPa), P2 after a given time at selected pressure, *etc.*

scattering vector, and finally $S(q)$ is the structure factor describing any interactions between particles. For a dilute system $S(q) = 1$.

The final model expression contains four contributions manifested on different length scales as outlined in Ingham et al. (2016) and illustrated in Fig. 2: (i) Population 1 (pop 1)—the overall casein micelles around 100 nm in size, (ii) Population 2 (pop 2)—internal water-separated micellar regions approximately 20 nm in size, (iii) Population 3 (pop 3)—protein structures which are inhomogeneous on a 1–3 nm length scale, and (iv) CCP particles 2–3 nm in size showing a correlation peak around $q = 0.035$ Å^{-1} (referred respectively as pop 4). However, as mentioned above, the CCP signal is usually not visible in SAXS experiments and we only found it necessary to include this term for the data obtained at 60 °C.

The overall micelles (pop 1), internal micellar regions (pop 2) and

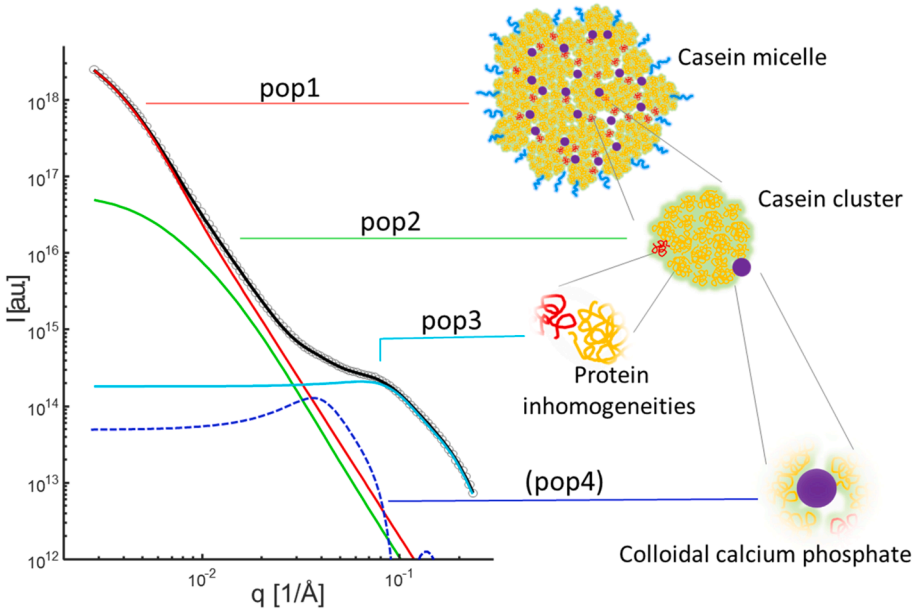

Fig. 2. Graphic representation of the four contributions of the model at different length scales, based on Ingham et al. (2016), representing: the overall casein micelles around 100 nm in size (pop 1); the internal water-separated micellar regions approximately 20 nm in size (pop 2); the protein structures which are inhomogeneous on a 1–3 nm length scale (pop 3); and CCP particles 2–3 nm in size (pop 4).

the CCP particles (pop 4) are modelled as polydisperse sphere distributions:

$$P_{PS}(q) = \int P_S(q)D(R)V(R)^2 dR \quad (2)$$

With the monodisperse sphere form factor given by

$$P_S(q) = \left[3\frac{sinqR - qRcosqR}{(qR)^3}\right]^2 \quad (3)$$

And the log-normal distribution by

$$D(R) = \frac{1}{R\sigma\sqrt{2\pi}} exp\left(\frac{-[ln(R/R_0)]^2}{2\sigma^2}\right) \quad (4)$$

where σ is the variance and R_0 is the geometric mean of the log-normal distribution; $V(R)$ is the sphere volume and R is radius of the spheres. The modelling of the small length scale protein scattering contribution (pop 3) follows Sørensen, Pedersen, Mortensen, and Ipsen (2013) using a modified Debye-Büche term.

$$P(q, \xi, \sigma_{DB}) = \frac{1}{1 + (q\xi)^2} exp\left(-\sigma_{DB}^2 q^2\right) \quad (5)$$

where ξ is a correlation length and σ_{DB} is a measure of the surface roughness. Both the CCP particle and the last protein contributions have an associated hard-sphere structure factor controlled by two parameters, an interaction radius R_{HS} and the volume fraction η. However, unlike Ingham et al. (2016) we do not include polydispersity in the Debye-Büche term. Since the scattering data are not obtained on an absolute intensity scale, each contribution to the final model intensity is scaled by a constant ci, i = 1,2,3,4. Assuming unchanged contrast of the incompressible water phase during pressure treatments, these constants become qualitative indicators for an increasing or decreasing number of particles of any particular contribution to the overall scattering.

The fitting procedures were performed using MATLAB ® R2018b (Mathworks, Inc., Matick, MA, USA) code, which at present does not evaluate deviations of the parameters internally. Independent fits to replicate samples revealed standard deviations (SD) < 1%. However,

Table 1
Parameters of pop3 from the fit of the SAXS data upon different HP processes of 200 MPa or 400 MPa treatments at 25 °C, for characterizing the properties of "protein inhomogeneities".

Data collection points		Scale factor ($c3$) [$\times 10^4$]	Correlation length (ξ_3) [nm]	Surface roughness (σ_{DB}) [Å]	Volume fraction (η_3)	Interaction radius (R_{HS3}) [nm]
HP Process 1 at 200 MPa	Point 0	5.35	1.59	5.46	0.107	3.32
	Point 1 (HP)	3.59	1.72	5.22	0.096	3.83
	Point 2 (HP)	2.61	1.81	4.33	0.067	3.97
	Point 3	4.19	1.39	5.89	0.085	3.38
	Point 4	7.06	1.98	4.45	0.119	3.28
	Point 5	7.96	2.11	5.04	0.127	3.21
HP Process 1 at 400 MPa	Point 0	6.63	1.61	5.38	0.088	3.24
	Point 1 (HP)	2.22	1.67	5.04	0.109	10.92
	Point 2 (HP)	1.92	1.72	4.80	0.165	13.57
	Point 3	5.71	1.44	6.16	0.047	3.42
	Point 4	5.18	1.17	6.37	0.091	3.83
	Point 5	5.42	1.21	6.14	0.089	3.79
HP Process 2 at 200 MPa	Point 0	4.70	1.57	5.62	0.107	3.25
	Point 1 (HP)	3.52	1.79	5.17	0.097	3.78
	Point 2 (HP)	2.08	1.85	3.41	0.079	4.10
	Point 3 (HP)	1.73	1.73	4.18	0.076	3.99
	Point 4	3.86	1.62	4.28	0.093	3.24
	Point 5	6.15	2.10	4.52	0.118	3.11
	Point 6	6.89	2.21	4.91	0.125	3.05
HP Process 3 at 200 MPa	Point 0	4.34	1.24	6.22	0.100	3.46
	Point 1 (HP)	4.30	1.89	4.30	0.095	3.79
	Point 2 (HP)	3.32	2.01	4.12	0.056	3.76
	Point 3	3.90	1.31	6.22	0.083	3.44
	Point 4 (HP)	3.08	1.84	5.02	0.057	3.75
	Point 5 (HP)	2.34	1.61	5.06	0.061	3.97
	Point 6	3.82	1.32	6.02	0.080	3.47
HP Process 3 at 400 MPa	Point 0	7.92	1.78	5.27	0.085	3.19
	Point 1 (HP)	2.61	1.79	5.05	0.139	11.24
	Point 2 (HP)	1.92	1.71	4.86	0.143	12.43
	Point 3	10.08	2.43	5.25	0.073	3.37
	Point 4 (HP)	2.13	1.86	4.72	0.137	12.39
	Point 5 (HP)	2.05	1.80	4.68	0.128	12.59
	Point 6	10.93	2.62	5.07	0.076	3.4

given the complexity of the system and the general resolution of SAXS we estimate the SD to be < 10% on the fitted parameters listed in tables 1 and 2 (Larsen, Arleth, & Hansen, 2018).

3. Results and discussion

3.1. Effect of pressure on milk structure during HP treatment

After background-subtraction, the skimmed milk SAXS data over a wide q-range during HP process 1 at 25 °C are shown in Fig. 3 (200 MPa) and Fig. 4 (400 MPa). In these processes, milk is held at 200 or 400 MPa for 5 min and the stability of the structure was followed after depressurization for up to 10 min. The data are presented in both log $I(q)$—log q and as log $[q^2 \cdot I(q)]$—log q (Kratky) plots and are generally consistent with SAXS patterns previously reported (Bouchoux et al., 2010; Ingham et al., 2016; Yang et al., 2018). Data were fitted well with the three-population model adapted from Ingham et al. (2016), as shown in Fig. 3 and Fig. 4. Comparing with the skimmed milk before HP (Fig. 3A), the scattering curves at low-q (around 0.2 $Å^{-1}$) gradually decreased in intensity indicating that the casein micelles have been dissociated under HP (Fig. 3B and C), leading to an increase of pop 2 (observed at intermediate-$q \sim 0.01$ $Å^{-1}$) *i.e.* micellar regions approximately 20 nm in size. Meanwhile, the high-q feature (0.08–0.2 $Å^{-1}$) of pop 3 consisting of protein inhomogeneities becomes flatter under pressure, suggesting that this structural domain becomes more uniform at HP, which applies throughout this study. Also, releasing the pressure (Fig. 3D, E, F) and comparing with the Kratky plots of the milk before HP (Fig. 3A), we observe that changes on high-q region are reversible. At 400 MPa, similar trends are observed, but all changes are more pronounced (Fig. 4). The overall scattering intensities $I(q)$ decreased even more when 400 MPa is applied (Fig. 4B, C) compared with non-pressurised milk (Fig. 4A) and 200 MPa (Fig. 3B, C). Under 400 MPa, the scattering curve becomes almost linear in the full q-range. Additionally, the intermediate-q feature (at 0.02 $Å^{-1}$, pop 2) became more noticeable at 400 MPa (Fig. 4C) as a consequence of dissociation of micelles from pop 1 into smaller "submicelles" (pop 2). Previously, Yang et al. (2018) observed a noticeable increase in intensity at intermediate-q at pressure above 270 MPa, and disappearance of high-q features with the increased pressure, which is also observed in our results.

Further analysis of the scattering curves show the appearance of isosbestic points in the scattering patterns, *i.e.* points which remain unchanged in intensity at a specific q-value (Tromp, Huppertz, & Kohlbrecher, 2015; Yang et al., 2018; Singh et al., 2020). An isosbestic point indicates the presence of structural features on either side of the point which remain largely unchanged in size but over time change their number ratio (Yang et al., 2018). We observe an isosbestic point at 200 MPa at 0.032 $Å^{-1}$ which is similar to Yang et al. (2018) reporting 0.030 $Å^{-1}$ and Singh et al. (2020) reporting 0.035 $Å^{-1}$, but the isosbestic point at 400 MPa is at 0.049 $Å^{-1}$ indicating a shift in size of the structural division of the colloidal units. Combining our results with these previous reports (Müller-Buschbaum et al., 2007; Ingham et al., 2016; Yang et al., 2018), we confirm that the pop 2 represents small casein clusters, not only from the inhomogeneous internal structure of casein micelles, but also from individual "mini-micelles" without CCP connection, previously termed "submicelles" (Pessen, Kumosinski, & Farrell, 1989).

Analyzing in more detail the parameters obtained from the modelling, the particle size distribution of micelles (pop 1) and submicelles (pop 2) are shown in Fig. 5 obtained from modelling the SAXS patterns of Figs. 3 and 4. It is generally accepted that casein micelles are polydisperse structures, with sizes ranging between 20 and 600 nm dependent on the environmental conditions (Marchin et al., 2007). The fitting of our SAXS data of untreated milk show size distributions ranging from 20 to 250 nm, well in agreement with expected values. As shown in Fig. 5A, when the pressure of 200 MPa is applied, both micelles and submicelles sizes are reduced. Especially the size distribution of pop 2 was reduced from a broad range to a quite narrow one (right subplot of Fig. 5A). Meanwhile, the number of micelles and submicelles both decrease indicating some bound caseins have been released to the serum by HP. When holding the HP at 200 MPa for 5 min, the number of micelles, pop 1 was significantly reduced and the number of pop 2 increased. It seems the large micelles from pop 1 have been dissociated into smaller micelles (pop 2) which agrees with previous reports that when HP approaches 200 MPa solubilization of CCP and micelle dissociation will occur (Olsen & Orlien, 2016). After depressurization and relaxation time at ambient pressure (point 3 to 5, in Fig. 5A), casein micelles sizes start to recover, leading to a slightly broader size distribution than before HP treatment. Furthermore, the number of micelles (pop1) and the size distribution of pop 2 were only partially reversed after the pressure was released in line with previous studies Olsen and Orlien (2016) and Yang et al. (2018). It reveals that there were more "submicelles" re-associated after HP treatment at 200 MPa and 25 °C for 5 min.

At 400 MPa, the casein micelle size and number were more strongly reduced, and when 400 MPa was reached (point 1), changes in pop 1 and 2 were immediately observed. After pressure releasing (point 3–5, Fig. 5B), the casein micelle and submicelles size distribution were not reverted within the time of our measurements. The number of large micelles almost reverted to the initial level, but the number of submicelles (pop 2) was clearly higher than before HP treatment. These results indicated that 400 MPa hinders the disrupted micelles to reorganize fully back to large micelles, which is presumably due to casein micelles associated with denatured β-Lg (Huppertz et al., 2002). Besides, it also revealed that the sudden depressurisation from 400 MPa splits the internal micellar regions (or submicelles) into a smaller size.

Table 2
Parameters from the fit of SAXS data upon HP Process 1 treatments under 200 MPa at 40 and 60 °C for characterizing the properties of protein inhomogeneities (pop 3) and CCP (pop 4).

Population parameters		At 40 °C						At 60 °C					
		P0	P1 (HP)	P2 (HP)	P3	P4	P5	P0	P1 (HP)	P2 (HP)	P3	P4	P5
Pop 3: protein	Scale factor ($c3$) [$\times 10^4$]	4.60	3.20	2.34	4.33	6.97	6.91	4.65	2.97	2.61	4.08	4.49	4.40
	Correlation length (ξ_3) [nm]	1.27	1.38	1.41	1.29	1.82	1.77	1.23	1.19	1.20	1.08	1.10	1.05
	Surface roughness (σ_{DB}) [Å]	6.05	5.82	4.81	6.20	5.22	5.42	5.69	5.55	5.40	6.38	6.39	6.47
	Volume fraction (η_3)	0.101	0.096	0.096	0.100	0.102	0.102	0.116	0.070	0.136	0.127	0.128	0.127
	Interaction radius (R_{HS3}) [nm]	3.38	3.87	3.99	3.41	3.23	3.21	3.18	3.60	3.64	3.48	3.46	3.47
Pop 4: CCP	Scale contrast ($c4$) [$\times 10^4$]	–	–	–	–	–	–	6.87	6.55	4.25	5.90	6.42	7.09
	Volume fraction (η_4)	–	–	–	–	–	–	0.186	0.086	0.163	0.179	0.170	0.192
	Interaction radius (R_{HS4}) [nm]	–	–	–	–	–	–	7.71	8.79	12.52	7.23	7.28	7.39
	[1] Particle radius (ξ_4) [nm]	–	–	–	–	–	–	4.15	3.37	4.62	4.58	4.58	4.50
	R_4	–	–	–	–	–	–	41.25	33.52	46.00	45.55	45.54	44.74
	σ_4	–	–	–	–	–	–	0.016	0.027	0.014	0.020	0.018	0.020

[1] Particle radius of CCP was the maximum of particle size distribution defined by both of R_4 and σ_4 parameters as *Size distrubution* = exp (log (R_4) - σ_4^2).

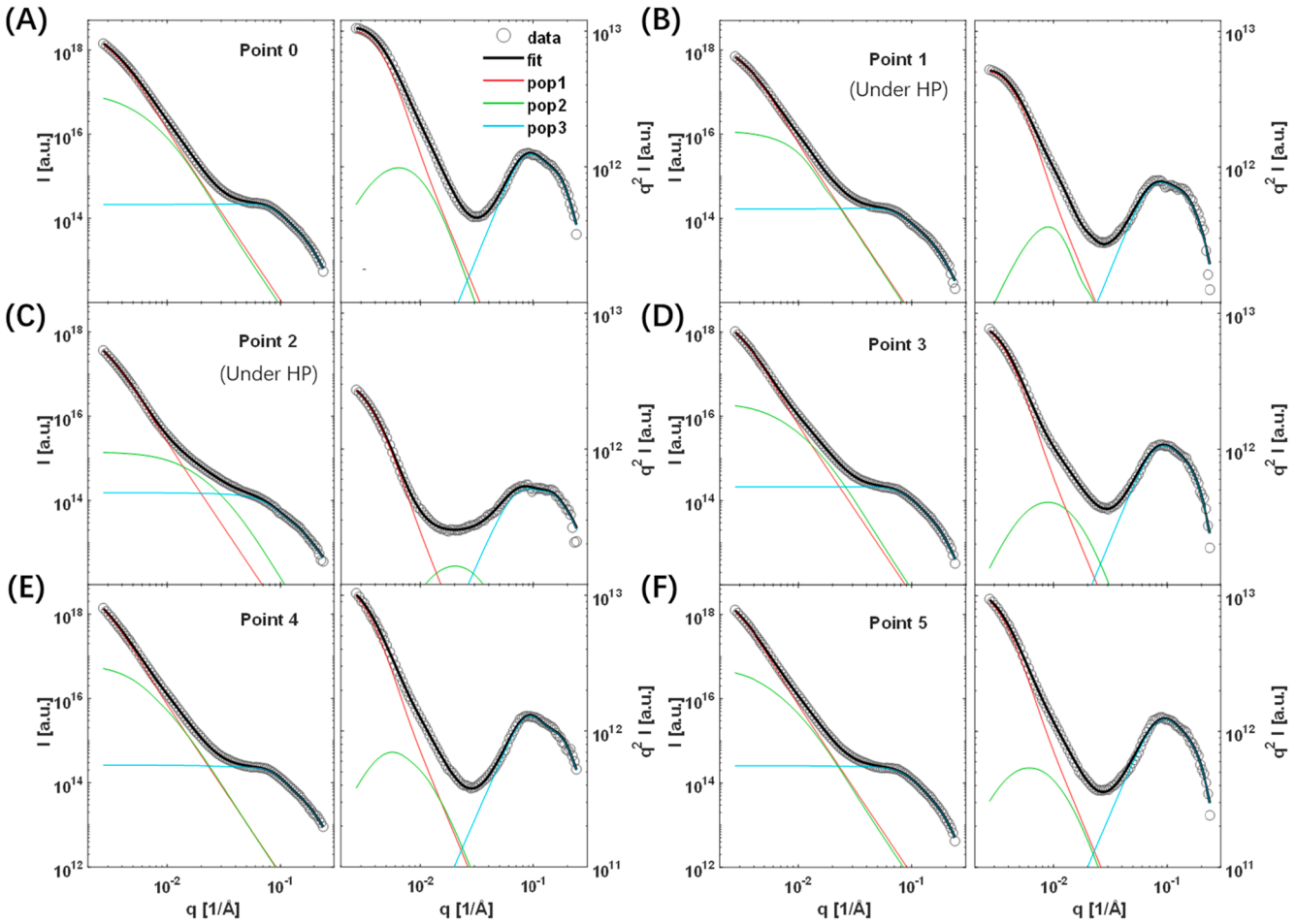

Fig. 3. Scattering curves from skimmed milk at 200 MPa at 25 °C upon HP process 1 fitted with three populations in both log–log (left) and Kratky (right) plots; (**A**) at P0 (before HP), (**B**) at P1 (immediately after reaching 200 MPa); (**C**) at P2 (after 5 min at 200 MPa); (**D**) at P3 (immediately after depressurization); (**E**) at P4 (5 min after depressurization); (**F**) at P5 (10 min after depressurization).

Limited studies are available regarding the "protein inhomogeneties", and we hypothesize they represent for example, whey protein aggregates, casein aggregates or casein-whey protein aggregates probably some mediated by calcium. The fitting of pop 3, with length scales between 1 and 3 nm, generates several parameters that provide more detailed structural information about this population named "protein inhomogeneties" (in Table 1). The scaling factor c_3 can roughly reflect the number of "protein inhomogenities" (protein aggregates). Correlation length ξ_3 of scatterers accounts for the scattering from protein strands, roughly reflecting the scatterers size. The parameter σ_{DB} is a measure of the roughness of pop3, denoting the surface fractal character. The interaction radius R_{HS3} is the radius between two scatterers reflecting the particle interaction distance. The volume fraction of η_3 reflects the interaction strength (*e.g.* the noncovalent hydrophobic, electrostatic interactions and hydrogen bonds) between scattering particles. Although, careful interpretation is needed because many parameters are fitted at same time and therefore the model in this region might be slightly over-parametrized, by tracking the alteration of these parameters, some nanostructural changes in this region caused by HP are characterizable. We will pursue at more comprehensive understanding of changes on this length scale in future work.

3.2. *Effect of holding time on milk structure dynamics during HP treatments at 200 MPa*

The total holding time of HP treatment at 200 Ma was prolonged to 10 min to understand the consequences of time at a given pressure on structure changes at low pressures. Comparing with the scattering curves in which HP was held for 5 min (Fig. 3), the high-q feature (around 0.1 $Å^{-1}$, pop 3) in HP process 2 held for 10 min became flatter and after releasing the pressure the intermediate-q feature around 0.01 $Å^{-1}$, pop 2, became more prominent. The parameters of the model fitted to the three populations are shown in Fig. 6 and Table 1. The structural differences between 5 min and 10 min is a more pronounced micelle disruption at 10 min leading to smaller micelle size (Fig. 6A). However, the overall size distribution of the micelles was broader and some larger size micelles were formed under HP (point 3). Thus, holding the HP for 10 min at 200 MPa may allow the disrupted small sized micelles to re-aggregate again to form some larger micelles. After releasing the pressure, both the micelles and submicelles were disrupted again into smaller sizes with a much narrower size distribution, and they did not revert any more throughout the relaxation time of 10 min at atmospheric pressure. This differs from HP processing for 5 min where both the size of micelle and submicelle could partially recover after releasing pressure, and HP processing for 5 min even induced some micelle aggregation when milk was under atmospheric pressure (Fig. 5A point 5). Previous results by *in situ* turbidimetry have shown that the casein micelles would dissociate at initial 10 min of HP treatment (50–500 MPa), but under pressure of 250–300 MPa for times longer than 10 min the dissociated submicelles would re-associate again into micelles with even larger size than before HP treatment (Orlien, Knudsen, Colon, & Skibsted, 2006). This is in line with what we observed with HP process 1 and 2 at 200 MPa.

Although after HP treatment at 200 MPa for 10 min led a comparable

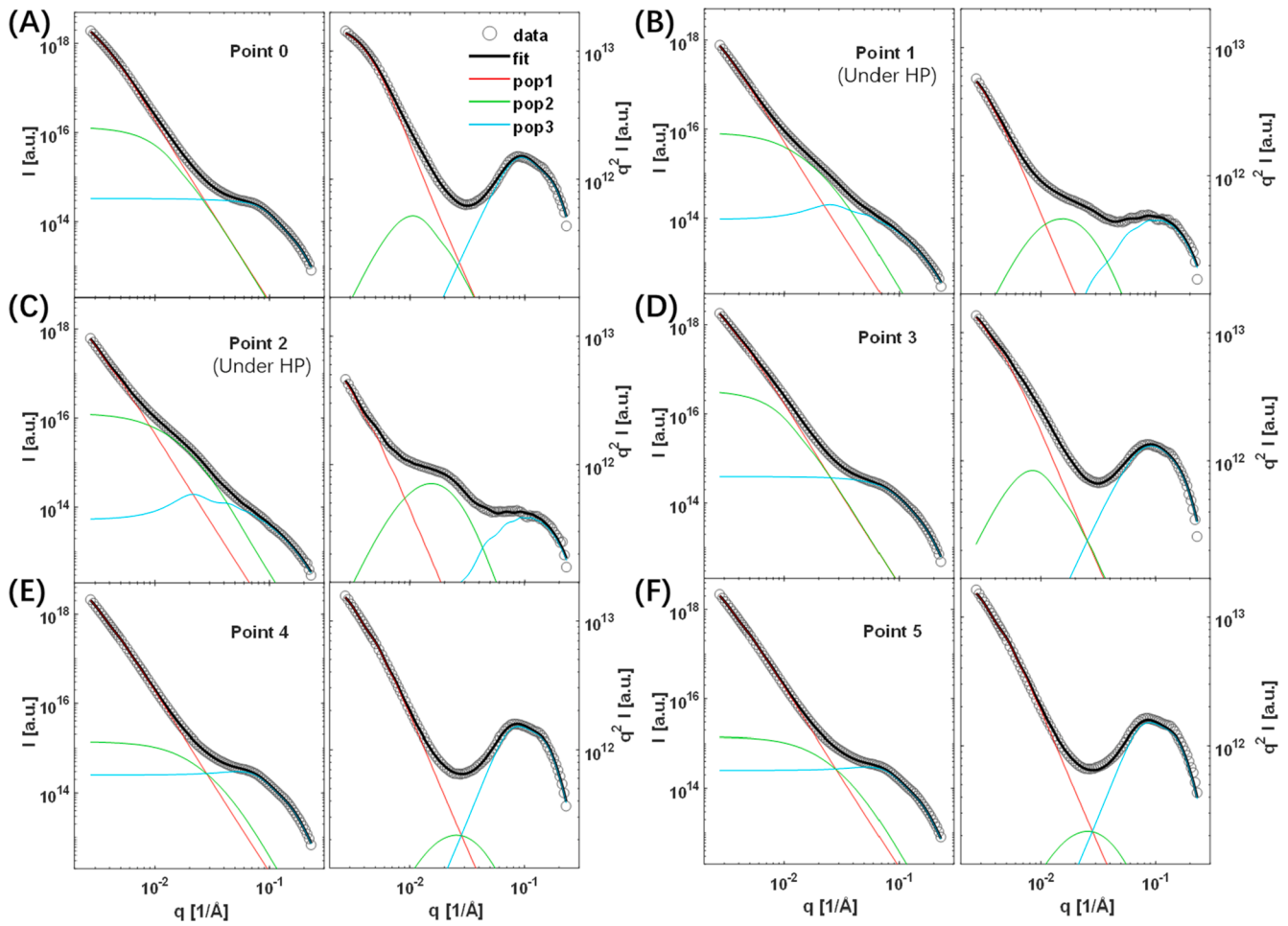

Fig. 4. Scattering curves from skimmed milk under 400 MPa at 25 °C upon HP process 1 fitted with three populations in both log–log (left) and Kratky (right) plots. (**A**) at P0 (before HP), (**B**) at P1 (immediately after reaching 400 MPa); (**C**) at P2 (after 5 min at 400 MPa); (**D**) at P3 (immediately after depressurization); (**E**) at P4 (5 min after depressurization); (**F**) at P5 (10 min after depressurization).

decreasing of pop 1 and pop 2 with treatment at 400 Ma for 5 min, for the dynamics of the pop 3 structure change in samples 200 MPa treated for 10 min is completely consistent with 5 min. The structural changes in this region are more pressure-dependent than time dependent, as at 400 MPa we observed irreversible changes in pop 3 that are not observed with the increase of time at 200 MPa.

3.3. *Effect of temperature on milk structure dynamics during HP treatment at 200 MPa*

The SAXS scattering curves for HP process 1 (200 MPa; 5 min) were compared at 20, 40 and 60 °C. At 40 °C scattering curves were well fitted with the three populations (pop 1, pop 2 and pop 3), but the scattering curves at 60 °C required the fourth population (pop 4). As shown in Fig. 7, a new scattering feature around 0.035 Å that arises from the CCP scattering (Ingham et al., 2015; 2016) was observed at 60 °C already in the milk before starting the HP process but disappeared when the HP was applied. Previous studies reported that increasing temperature facilitates the CCP formation (Aoki, Umeda, & Kako, 1990; Liu, Weeks, Dunstan, & Martin, 2013) as calcium phosphate solubility decreases with increasing temperature (On-Nom, Grandison, & Lewis, 2010), but increases with pressure increase (Schrader, Buchheim, & Morr, 1997; Huppertz et al., 2002). The fitted results and parameter details are shown in Table 2 and Fig. 8. Compared to at 25 °C, the casein micelle size at 40 °C was less reduced by HP treatment and the size did not revert after releasing the pressure. Notably, the number of micelles after HP treatment at 40 °C increased whilst at 25 °C the number tended to decrease. However, the size of pop 2 for casein clusters at 40 °C was reduced under HP, but reverted to a broader size distribution after releasing the pressure. HP treatment at 40 °C led more soluble caseins associating/assembling to clusters, which might be ascribed to the increasing strength of hydrophobic bonds at higher temperature (Moitzi, Portnaya, Glatter, Ramon, & Danino, 2008; Beliciu & Moraru, 2009), and they are more easily associated with other whey proteins hindering the submicelles aggregation and micelle reformation. At 60 °C, the micelles and submicelle dynamics is completely different. HP treatment increased the casein micelle size and its size did not shrink back after releasing pressure (Fig. 8B). Dalgleish, Pouliot, and Paquin (1987) studied the effect of heat treatment of milk on casein micelle size, and were able to show effectively that micelle size increased because of aggregation of κ-casein and serum proteins in agreement with our observation. Meanwhile the number of submicelles after HP treatment at 60 °C appears effectively constant although shrinking irreversibly in size, unlike the number of pop 2 at 25 and 40 °C, which returned to the original size.

As shown in Table 2, the variation of most fitted parameters for pop 3 at 40 °C was similar to those at 25 °C but the volume fraction (η_3) related with the interaction strength of pop 3 was not lowered after HP holding for 5 min. It indicates that the temperature also affects on pop 3 interactions under HP. At 60 °C, the scattering features at high-q (0.08–0.2 $Å^{-1}$) were separated into two populations, "protein inhomogeneities" (pop 3) and CCP (pop 4). As mentioned, the scattering feature of CCP at $q = 0.035$ $Å^{-1}$ is normally not observed by SAXS (Ingham et al., 2016), but is commonly seen in small-angle neutron

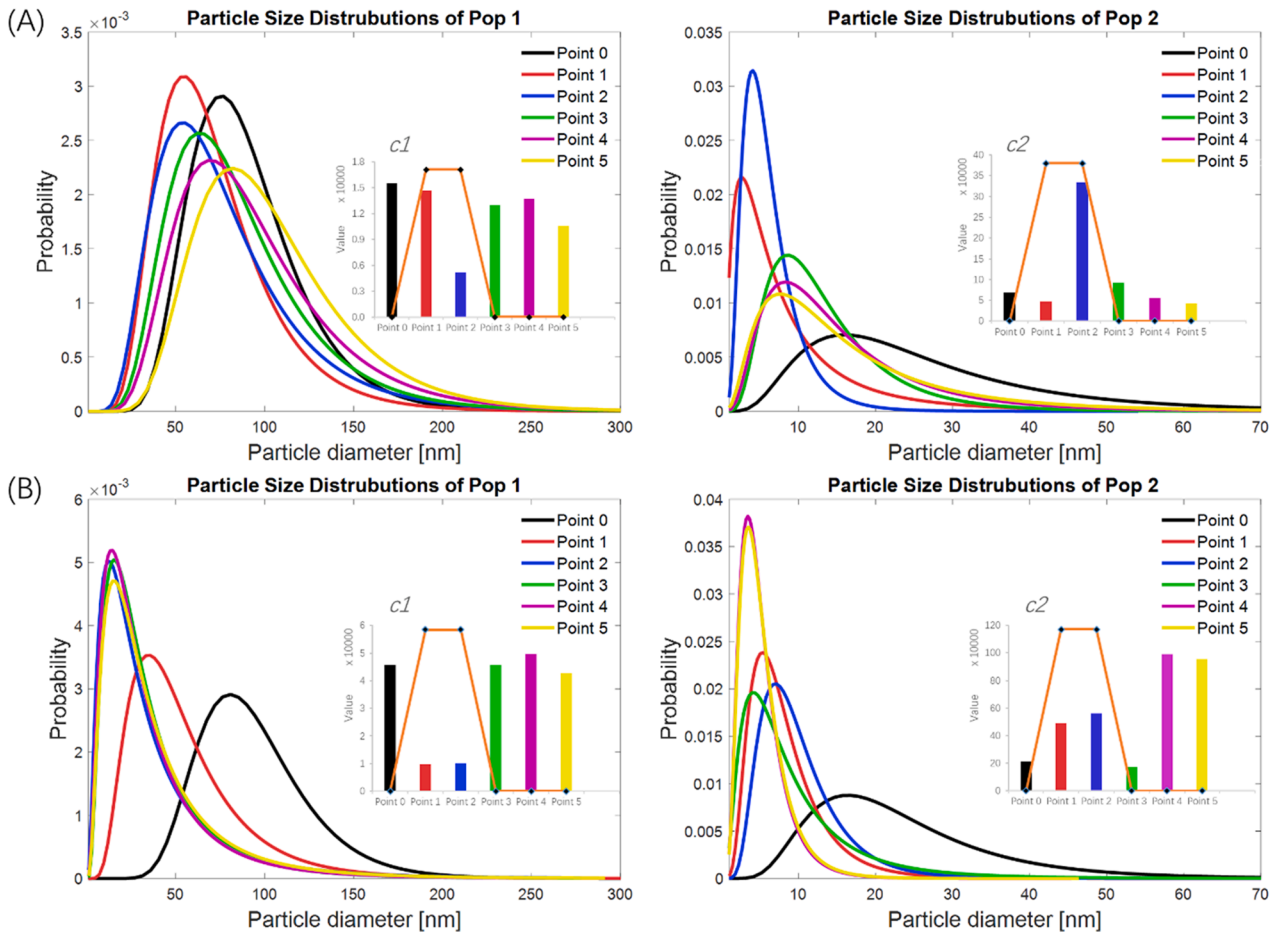

Fig. 5. Particle size distribution of population 1 (left) and population 2 (right) at different SAXS data collection points upon HP process 1 at 200 MPa (A) and 400 MPa (B) at 25 °C. Inserts are the parameter c1 and c2 reflecting number of scattering units of that population.

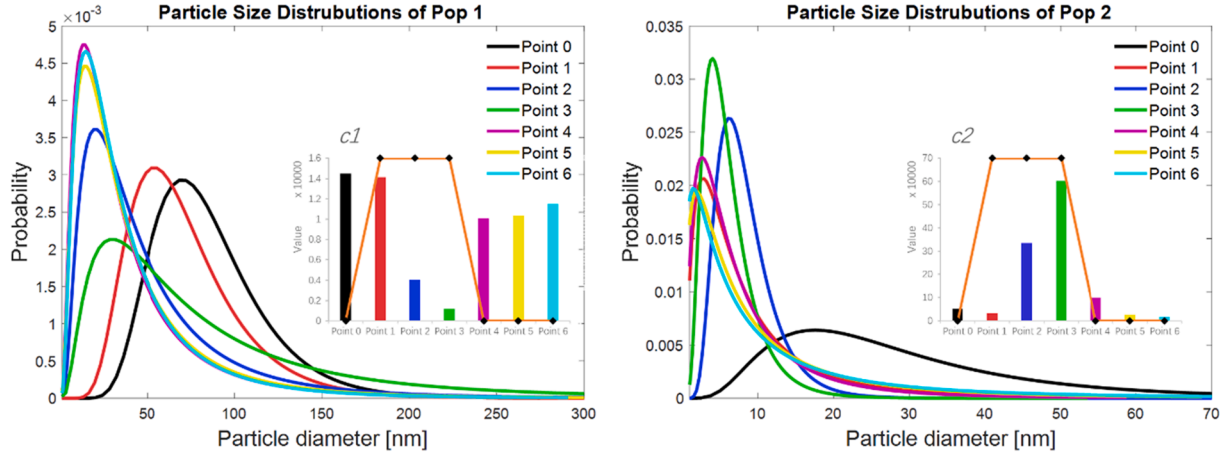

Fig. 6. Particle size distribution of population 1 (left) and population 2 (right) during HP process 2 at 200 MPa at 25 °C. Inserts are the parameter *c1* and *c2* reflecting number of scattering units of that population.

scattering (SANS) patterns (Hansen et al., 1996; Holt, de Kruif, Tuinier, & Timmins, 2003; Singh et al., 2020). In these studies, the radius of the CCP nanoclusters has been reported to be approx. 2–3 nm (Schrader et al., 1997; Ingham et al., 2016), although Singh et al. (2020) reported a radius of ~6 nm from SANS. In our study, the fitting results showed that CCP radius before HP processing was 4 nm, after reaching 200 MPa: 3 nm, after 5 min at 200 MPa: 5 nm and 4 nm after releasing the pressure. The values are within the range expected and give an idea of the CCP size dynamic evolution under HP treatment, confirming previous results suggesting that the HP-induced partial dissolution of CCP nanoclusters is reversible (Huppertz et al., 2002; Yang et al., 2018). Comparing the SAXS curves (Fig. 7), after HP treatment the CCP scattering feature is more prominent, and the CCP size also increased (Table 2) indicating the 200 MPa of HP treatment at 60 °C promoted the CCP formation, which could partly account for the casein micelle size increasing at 60 °C.

The dynamics of characteristic parameters of CCP (η_4 and R_{HS4}) were

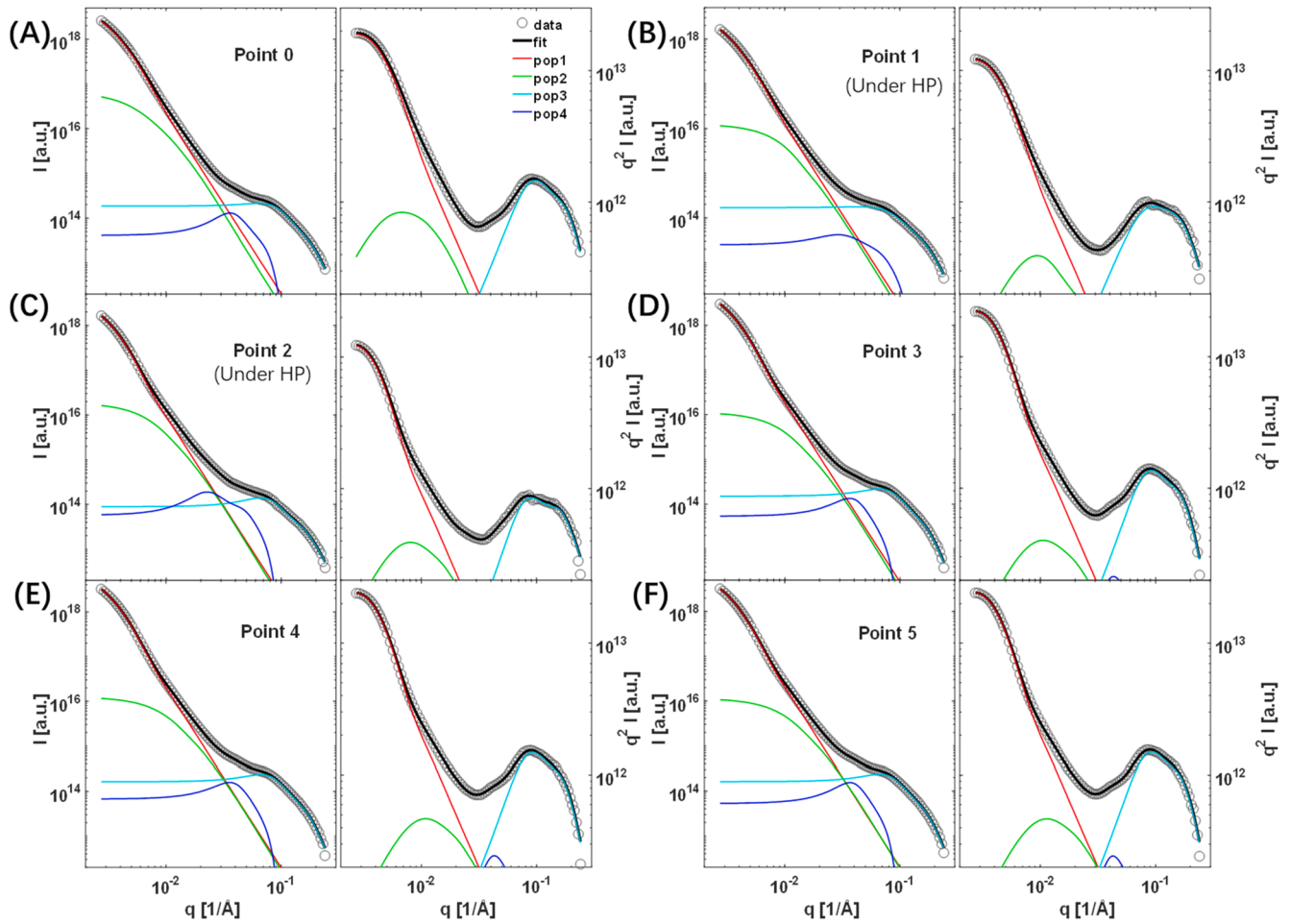

Fig. 7. Scattering curves from skimmed milk under 200 MPa at 60 °C during HP process 1 fitted with four populations in both log–log (left) and Kratky (right) plots. (**A**) at P0 (before HP), (**B**) at P1 (immediately after reaching 200 MPa); (**C**) at P2 (after 5 min at 200 MPa); (**D**) at P3 (immediately after depressurization); (**E**) at P4 (5 min after depressurization); (**F**) at P5 (10 min after depressurization).

consistent with protein inhomogeneities (Table 2). The number of scatterers, reflected by *c3* and *c4* variations were also similar at 25 and 40 °C, being lower under HP and reverting after HP treatment. However, the rest of the fitted parameters for protein inhomogeneities at 60 °C differ from 25 and 40 °C. Firstly, the protein particle correlation length ξ_3 decreases under HP and further decreases after HP processing. We speculate that the higher temperature of 60 °C combined with HP of 200 MPa disrupted the internal structure of protein inhomogeneities and the increasing hydrophobicity promote protein interactions. Secondly, although the protein surface roughness σ_{DB} decreases under HP, similarly to 25 and 40 °C, but after releasing the HP it increased, which was also observed at 400 MPa. Thirdly, the volume fraction η_3 reversibly became higher after HP was held for 5 min and after despressurisation η_3 increase was subtle, not like 200 MPa at 25 °C where an obvious increase after HP processing was observed.

In conclusion, increasing temperature during HP process at 200 MPa tends to facilitate casein protein association, but has more severe effects on "protein inhomogeneities" within the casein structure, leading to similar effects observed for milk pressurized at 400 MPa, at 25 °C, *e.g.* compressed protein particles (aggregation) causing the correlation length to decrease and increase protein surface roughness.

3.4. Effect of cycled treatment on milk structure dynamics

Previously, Yang et al. (2020) found differences in the physico-chemical properties of milk under cycled HP treatment in comparison to continuous HP treatment. Based on this work, we designed HP process 3 with a two cycle HP processing (2 × 2.5 min) instead of continuous HP processing for 5 min as in HP process 1. HP process 3 included a depressurization after 2.5 min and then re-pressurisation and a final 2.5 min HP treatment.

As shown in Table 1 and Fig. 9A, at 200 MPa the variations of these characteristic parameters for micelle size, submicelle size and protein structure were consistent with previous observations in HP process 1. Besides the size of pop 1 and 2, the fitted parameters for characterization of milk structure almost revert to the initial values after HP processing holding for 2.5 min at point 3. However, when the second cycle was applied the results differ from the first cycle. The first cycle of HP processing for 2.5 min caused effects that were not completely recovered before the second pressurization was applied. At the end of the process the number and size of micelles and submicelles variations are less changed than continuous HP processing. For example when releasing the pressure in the continuous process, the number of micelles was lower than before HP treatment while it was slightly higher than before HP treatment at the pressure releasing points (point 3 and 6) in cycled HP. When HP was held for a total of 5 min (point 2 in HP process1 and point 5 in HP process 3), the number of submicelles increased less and the size of micelle and submicelle decreased to less extent in HP process 3. This might be due to the cycled HP processing giving casein clusters a short break to re-associate and re-assemble.

The milk structure dynamics during HP process 3 at 400 MPa was almost similar with HP Process 1 at 400 MPa. Comparing the values at final depressurization of the milk (point 3 in HP process 1 and point 6 in HP process 3), we can see that at 400 MPa cycled HP treatment the

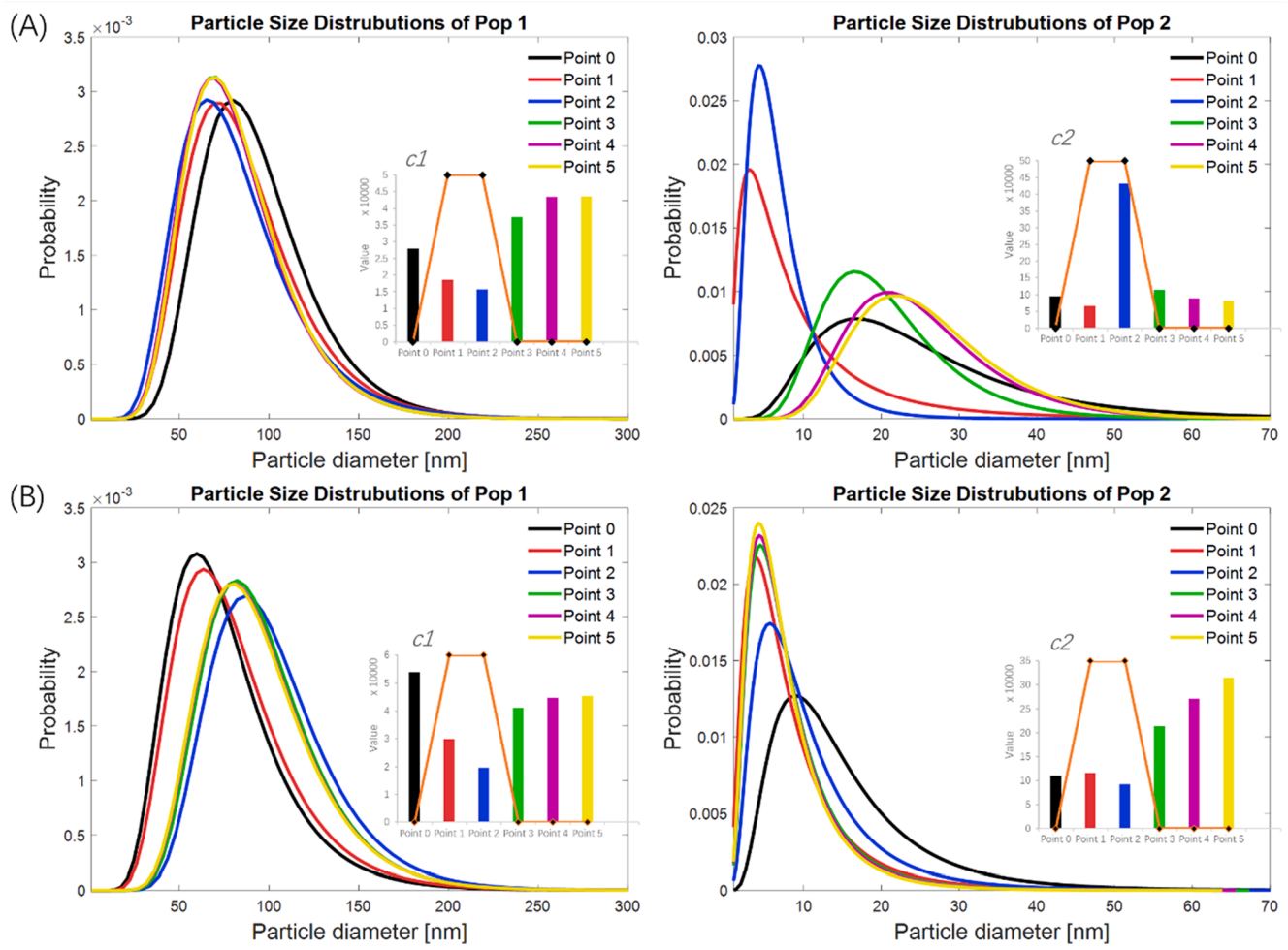

Fig. 8. Particle size distribution of population 1 (left) and population 2 (right) at different SAXS data collection points during HP process 1 under 200 MPa at 40 °C (**A**) and 60 °C (**B**). Inserts are the parameter *c1* and *c2* reflecting number of scattering units of that population.

reduction in the casein and submicelle size were more reversible than in the continuous HP processing. In the cycled process, the micelles that have been dissociated into smaller size did not revert after releasing pressure, but the micelle size reverses more after the second cycle (point 6 in Fig. 9B). Previously, it was also found the casein micelle size to be slightly larger after a two-cycle HP treatment (2 × 2.5 min) than a continued HP treatment (1 × 5 min) at 600 MPa by light scattering measurement (Yang et al., 2020). In the case of pop 2, the size of submicelles recovered but was still below the initial level of continuous HP processing (Fig. 4B). Moreover, we also observed that the correlation length ξ_3 was abnormally higher at the pressure releasing points (point 3 and 6) in HP process 3, this was only found at higher pressure and lower temperature (400 MPa at 25 °C). During HP treatment tests, we found that the depressurisation process may cause milk volume expansion which may explain the large ξ_3 value. This might be due to the water molecules being forced into the proteins by pressure (Cadesky, Walkling-Ribeiro, Kriner, Karwe, & Moraru, 2017) at lower temperature, and a fast depressurisation caused expansion of the protein structure due to hydration. Releasing the pressure step-by-step might avoid this phenomenon. Nevertheless, cycled HP processing has effects on the submicelles and micelles, allowing casein re-association thus decreasing the total HP effects on their size.

4. Conclusions

This study demonstrates the potential use of synchrotron SAXS coupled with HP to examine *in situ* the structural dynamics of milk during different HP treatments. The model proposed by Ingham et al. (2016) showed to be adequate to describe the data using three contributions on different length scales. The data analysis provides insight on changes in casein micelles and their internal structure. Our results show that the hierarchical structure of milk at various length scales is affected by pressure, time, temperature and repeated pressurisation (cycles) during HP treatments, and that some changes are partially reversible or irreversible after the pressure is released. The results confirm that increased pressure caused solubilization of CCP and dissociation of casein micelles into smaller sized casein clusters, and also showed modification of nanoscale protein inhomogeneties (pop 3, 1–3 nm length). Temperature during the HP process has a major effect on the nanostructure of milk. Below 40 °C the scattering curves were well fitted with the three populations (pop 1, pop 2 and pop 3), while at 60 °C a fourth population (pop 4) representing CCP was required. The temperature increase to 60 °C at 200 MPa facilitated casein protein association, but has more severe effects on "protein inhomogeneities" within the casein structure, leading to similar effects observed for milk pressurized at 400 MPa. Under HP, the increasing of process time induced re-aggregation of micelles that was not observed for shorter process times, however, changes in protein nanostructures were more pressure-dependent than time dependent. Furthermore, our results showed that casein micelles and the structure of micellar internal regions are more reversibly re-associated after cycled treatment, which has implications for the physical properties of milk.

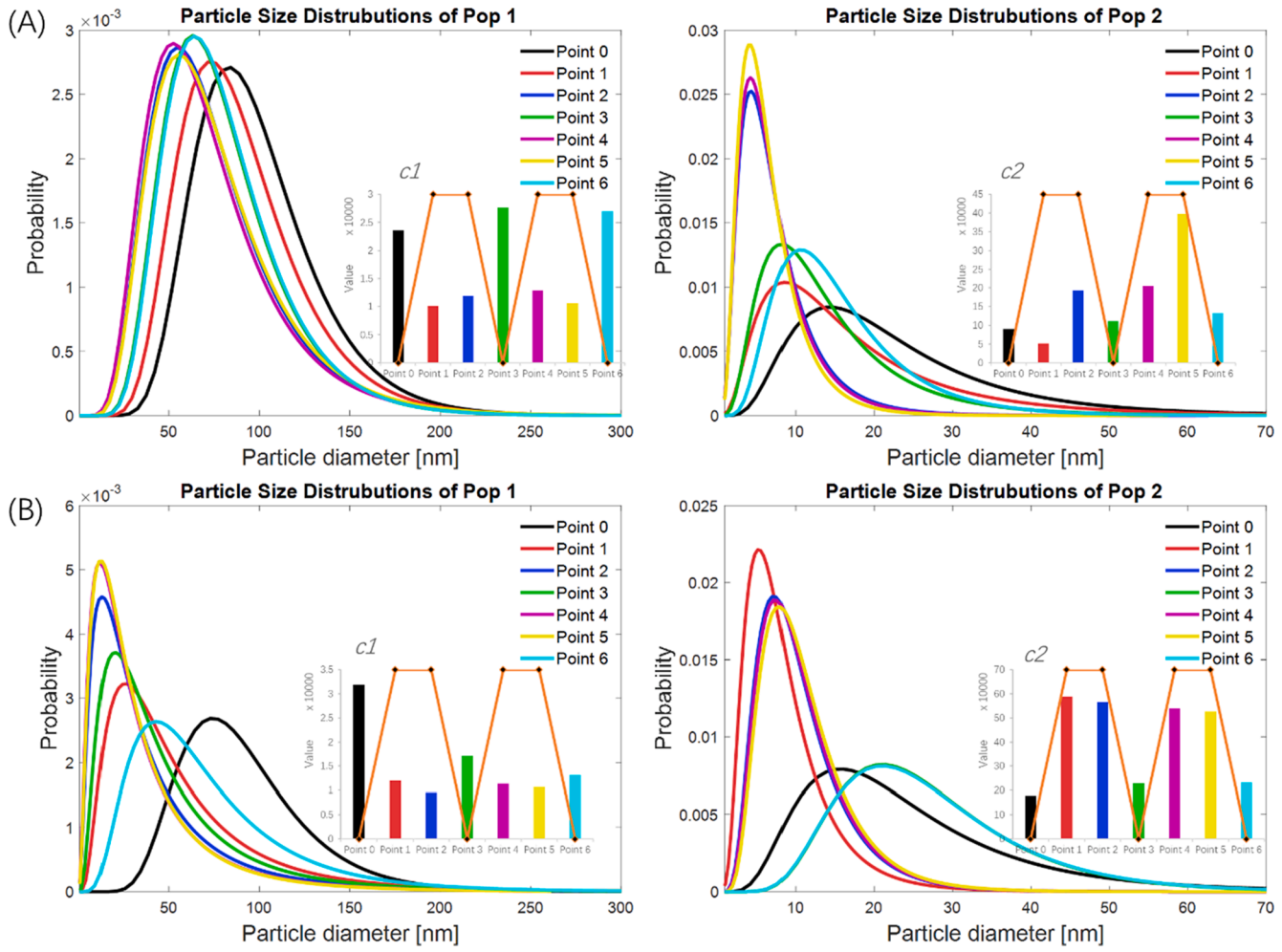

Fig. 9. Particle size distribution of population 1 (left) and population 2 (right) during HP process 3 for HP cycle-treatment at 25 °C under 200 MPa (**A**) and 400 MPa (**B**). Inserts are the parameter *c1* and *c2* reflecting number of scattering units of that population.

CRediT authorship contribution statement

Shuailing Yang: Conceptualization, Investigation, Methodology, Writing - original draft. **Arwen I.I. Tyler:** Conceptualization, Investigation, Methodology, Writing - review & editing. **Lilia Ahrné:** Conceptualization, Methodology, Investigation, Supervision, Writing - original draft, Writing - review & editing. **Jacob J.K. Kirkensgaard:** Conceptualization, Investigation, Methodology, Writing - review & editing.

Declaration of Competing Interest

The authors declare that they have no known competing financial interests or personal relationships that could have appeared to influence the work reported in this paper.

Acknowledgments

We thank Diamond Light Source for the award of synchrotron beamtime (SM24374), Dr. Olga Shebanova and Prof. Nick Terrill for their support and assistance. We also thank Dr. Aleks Ponjavic from the University of Leeds for valuable help in performing the SAXS measurements. The Bragg Centre for Materials Research at the University of Leeds is also acknowledged. The present study was financially supported by the Dairy Rationalization Fund (DDRF), Arla Foods amba, the Innovation Fund Denmark through the FAPESP project Novel Aging – Technologies and solutions to manufacture novel dairy products for healthy aging (grant 2017/01189-0), and the Chinese Scholarship Council (grant 201706170082).

Appendix A. Supplementary material

Supplementary data to this article can be found online at https://doi.org/10.1016/j.foodres.2021.110527.

References

Aoki, T., Umeda, T., & Kako, Y. (1990). Cleavage of the linkage between colloidal calcium phosphate and casein on heating milk at high temperature. *Journal of Dairy Research, 57*(3), 349–354.

Beliciu, C. M., & Moraru, C. I. (2009). Effect of solvent and temperature on the size distribution of casein micelles measured by dynamic light scattering. *Journal of Dairy Science, 92*(5), 1829–1839.

Bouchoux, A., Gesan-Guiziou, G., Pérez, J., & Cabane, B. (2010). How to squeeze a sponge: Casein micelles under osmotic stress, a SAXS study. *Biophysical Journal, 99*(11), 3754–3762.

Boukria, O., El Hadrami, E. M., Boudalia, S., Safarov, J., Leriche, F., & Aït-Kaddour, A. (2020). The effect of mixing milk of different species on chemical, physicochemical, and sensory features of cheeses: a review. *Foods, 9*(9), 1309.

Brooks, N. J., Gauthe, B. L., Terrill, N. J., Rogers, S. E., Templer, R. H., Ces, O., et al. (2010). Automated high pressure cell for pressure jump x-ray diffraction. *Review of Scientific Instruments, 81*(6), Article 064103.

Cadesky, L., Walkling-Ribeiro, M., Kriner, K. T., Karwe, M. V., & Moraru, C. I. (2017). Structural changes induced by high-pressure processing in micellar casein and milk protein concentrates. *Journal of Dairy Science, 100*(9), 7055–7070.

Cornell, A. (2017). HPP Process for Dairy Foods, Patent application WO 2017/054052 Al.

Dalgleish, D. G., & Corredig, M. (2012). The structure of the casein micelle of milk and its changes during processing. *The Annual Review of Food Science and Technology, 3*, 449–467.
Dalgleish, D. G., Pouliot, Y., & Paquin, P. (1987). Studies on the heat stability of milk: II. Association and dissociation of particles and the effect of added urea. *Journal of Dairy Research, 54*(1), 39–49.
Day, L., Raynes, J. K., Leis, A., Liu, L. H., & Williams, R. P. W. (2017). Probing the internal and external micelle structures of differently sized casein micelles from individual cows milk by dynamic light and small-angle X-ray scattering. *Food Hydrocolloids, 69*, 150–163.
de Kruif, C. (2014). The structure of casein micelles: A review of small-angle scattering data. *Journal of Applied Crystallography, 47*(5), 1479–1489.
Hansen, S., Bauer, R., Lomholt, S. B., Quist, K. B., Pedersen, J. S., & Mortensen, K. (1996). Structure of casein micelles studied by small-angle neutron scattering. *European Biophysics Journal, 24*(3), 143–147.
Holt, C., de Kruif, C. G., Tuinier, R., & Timmins, P. A. (2003). Substructure of bovine casein micelles by small-angle X-ray and neutron scattering. *Colloids and Surfaces A: Physicochemical and Engineering Aspects, 213*(2–3), 275–284.
Hu, G., Zheng, Y., Wang, D., Zha, B., Liu, Z., & Deng, Y. (2015). Comparison of microbiological loads and physicochemical properties of raw milk treated with single-/multiple-cycle high hydrostatic pressure and ultraviolet-C light. *High Pressure Research, 35*(3), 1620–1635.
Hu, G., Zheng, Y., Liu, Z., & Deng, Y. (2017). Effects of UV-C and single- and multiple-cycle high hydrostatic pressure treatments on flavor evolution of cow milk: GC-MS, e-nose, and e-tongue analyses. *International Journal of Food Properties, 20*(7), 1677–1688.
Huppertz, T., Fox, P. F., de Kruif, K. G., & Kelly, A. L. (2006). High pressure-induced changes in bovine milk proteins: A review. *Biochimica et Biophysica Acta (BBA)-Proteins and Proteomics, 1764*(3), 593–598.
Huppertz, T., Kelly, A. L., & Fox, P. F. (2002). Effects of high pressure on constituents and properties of milk. *International Dairy Journal, 12*(7), 561–572.
Ingham, B., Erlangga, G. D., Smialowska, A., Kirby, N. M., Wang, C., Matia-Merino, L., et al. (2015). Solving the mystery of the internal structure of casein micelles. *Soft Matter, 11*(14), 2723–2725.
Ingham, B., Smialowska, A., Erlangga, G., Matia-Merino, L., Kirby, N., Wang, C., et al. (2016). Revisiting the interpretation of casein micelle SAXS data. *Soft Matter, 12*(33), 6937–6953.
Gaucheron, F., Famelart, M. H., Mariette, F., Raulot, K., Michela, F., & Le Graeta, Y. (1997). Combined effects of temperature and high-pressure treatments on physicochemical characteristics of skim milk. *Food Chemistry, 59*(3), 439–447.
Larsen, A. H., Arleth, L., & Hansen, S. (2018). Analysis of small-angle scattering data using model fitting and Bayesian regularization. *Journal of Applied Crystallography, 51*(4), 1151–1161.
Lopez, C., Briard-Bion, V., Ménard, O., Beaucher, E., Rousseau, F., Fauquant, J., et al. (2011). Fat globules selected from whole milk according to their size: Different compositions and structure of the biomembrane, revealing sphingomyelin-rich domains. *Food Chemistry, 125*(2), 355–368.
López-Fandiño, R. (2006). High pressure-induced changes in milk proteins and possible applications in dairy technology. *International Dairy Journal, 16*(10), 1119–1131.
Liu, G., Carøe, C., Qin, Z., Munk, D. M., Crafack, M., Petersen, M. A., et al. (2020). Comparative study on quality of whole milk processed by high hydrostatic pressure or thermal pasteurization treatment. *LWT, 127*, Article 109370.
Liu, D. Z., Weeks, M. G., Dunstan, D. E., & Martin, G. J. (2013). Temperature-dependent dynamics of bovine casein micelles in the range 10–40 °C. *Food chemistry, 141*(4), 4081–4086.
Mata, J. P., Udabage, P., & Gilbert, E. P. (2011). Structure of casein micelles in milk protein concentrate powders via small angle X-ray scattering. *Soft Matter, 7*(8), 3837–3843.
Marchin, S., Putaux, J. L., Pignon, F., & Léonil, J. (2007). Effects of the environmental factors on the casein micelle structure studied by cryo transmission electron microscopy and small-angle x-ray scattering/ultrasmall-angle x-ray scattering. *The Journal of Chemical Physics, 126*(4), Article 045101.
Moitzi, C., Portnaya, I., Glatter, O., Ramon, O., & Danino, D. (2008). Effect of temperature on self-assembly of bovine β-casein above and below isoelectric pH. Structural analysis by cryogenic-transmission electron microscopy and small-angle X-ray scattering. *Langmuir, 24*(7), 3020–3029.
Müller-Buschbaum, P., Gebhardt, R., Roth, S. V., Metwalli, E., & Doster, W. (2007). Effect of calcium concentration on the structure of casein micelles in thin films. *Biophysical Journal, 93*(3), 960–968.
Olsen, K., & Orlien, V. (2016). High-Pressure Processing for Modification of Food Biopolymers. In Innovative Food Processing Technologies (pp. 291-313). Woodhead Publishing.
On-Nom, N., Grandison, A. S., & Lewis, M. J. (2010). Measurement of ionic calcium, pH, and soluble divalent cations in milk at high temperature. *Journal of Dairy Science, 93*(2), 515–523.
Orlien, V., Knudsen, J. C., Colon, M., & Skibsted, L. H. (2006). Dynamics of casein micelles in skim milk during and after high pressure treatment. *Food Chemistry, 98*(3), 513–521.
Pedersen, M. C., Arleth, L., & Mortensen, K. (2013). WillItFit: A framework for fitting of constrained models to small-angle scattering data. *Journal of Applied Crystallography, 46*, 1894–1898.
Pessen, H., Kumosinski, T. F., & Farrell, H. M. (1989). Small-angle X-ray scattering investigation of the micellar and submicellar forms of bovine casein. *Journal of Dairy Research, 56*, 443–451.
Peyronel, F., Marangoni, A. G., & Pink, D. A. (2020). Using the USAXS technique to reveal the fat globule and casein micelle structures of bovine dairy products. *Food Research International, 129*, Article 108846.
Schrader, K., Buchheim, W., & Morr, C. V. (1997). High pressure effects on the colloidal calcium phosphate and the structural integrity of micellar casein in milk. Part 1. High pressure dissolution of colloidal calcium phosphate in heated milk systems. *Food/Nahrung, 41*(3), 133–138.
Singh, R., Hemar, Y., Gilbert, E.P., Wu, Z., & Yang, Z. (2020). Effect of genipin cross-linking on the structural features of skim milk in the presence of ethylenediaminetetraacetic acid (EDTA). Colloids and Surfaces A: Physicochemical and Engineering Aspects, 125174.
Sørensen, H., Pedersen, J. S., Mortensen, K., & Ipsen, R. (2013). Characterisation of fractionated skim milk with small-angle X-ray scattering. *International Dairy Journal, 33*(1), 1–9.
Spanos, N., Patis, A., Kanellopoulou, D., Andritsos, N., & Koutsoukos, P. G. (2007). Precipitation of calcium phosphate from simulated milk ultrafiltrate solutions. *Crystal Growth and Design, 7*(1), 25–29.
Smith, G. N., Brok, E., Christiansen, M. V., & Ahrné, L. (2020). Casein micelles in milk as sticky spheres. *Soft Matter, 16*(43), 9955–9963.
Tromp, R. H., Huppertz, T., & Kohlbrecher, J. (2015). Casein micelles at non-ambient pressure studied by neutron scattering. *Food Biophysics, 10*(1), 51–56.
Trujillo, A. J., Capellas, M., Saldo, J., Gervilla, R., & Guamis, B. (2002). Applications of high-hydrostatic pressure on milk and dairy products: A review. *Innovative Food Science & Emerging Technologies, 3*(4), 295–307.
Voigt, D. D., Kelly, A. L., & Huppertz, T. (2015). High-pressure processing of milk and dairy products. *Emerging Dairy Processing Technologies: Opportunities for the Dairy Industry, 1*, 71–92.
Walstra, P. (1999). Casein sub-micelles: Do they exist? *International Dairy Journal, 9*(3–6), 189–192.
Yang, S., Liu, G., Munk, D. M., Qin, Z., Petersen, M. A., Cardoso, D. R., et al. (2020). Cycled high hydrostatic pressure processing of whole and skimmed milk: Effects on physicochemical properties. *Innovative Food Science & Emerging Technologies, 102378*.
Yang, Z., Gu, Q., Banjar, W., Li, N., & Hemar, Y. (2018). *In situ* study of skim milk structure changes under high hydrostatic pressure using synchrotron SAXS. *Food Hydrocolloids, 77*, 772–776.